Production of HHH and HHV (V=γ, Z) at the hadron colliders[1]

Pankaj Agrawal, Debashis Saha[2], and Ambresh Shivaji

August 9, 2018

The First International High Energy Physics School and Workshop in Western China

[1]based on the paper: Phys. Rev. D 97, 036006 (2018)
[2]presenter : Institute of Physics, India

Outline

- Invariant Amplitude, and Cross-section
- Feynman Diagrams for our processes
- Anomalous Couplings
- $gg \rightarrow HHH$
- $gg \rightarrow HHZ$
- summary and conclusion

Invariant Amplitude, and Cross-section

- $d\hat{\sigma}_{ij\to\{f\}} = \frac{1}{(2E_i)(2E_j)|v_i - v_j|} d\Pi_n |\mathcal{M}|^2$ where

$$d\Pi_n = \left(\prod_f \frac{d^3 p_F}{(2\pi)^3} \frac{1}{2E_f} \right) (2\pi)^4 \delta^4 (p_i + p_j - \sum_f p_f)$$

- $\sigma_{AB\to\{f\}} = \sum_{i,j} \int dx_1 dx_2 d\hat{t} f^1_{i/A}(x_1, Q^2) f^2_{j/B}(x_2, Q^2) \frac{d\hat{\sigma}_{ij\to\{f\}}}{d\hat{t}}$,
- To find the value of integration and distribution, a parallel version program, AMCI (Advanced Monte Carlo Integration), which is based on VEGAS algorithm, has been used.

PDF
Parton Distribution Function

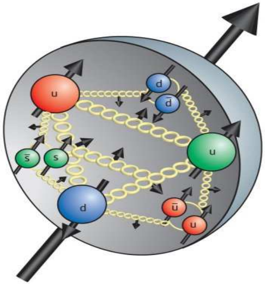

(a) Proton

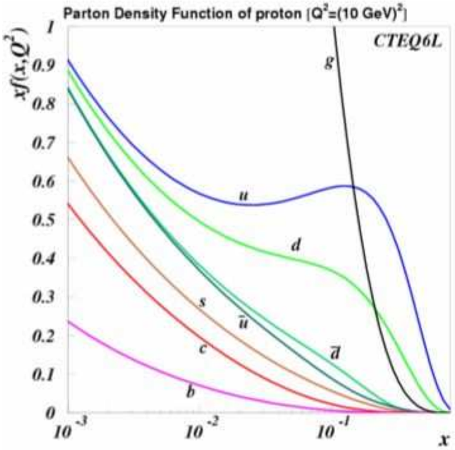

(b) Parton Distribution Function

Feynman Diagrams for Our Processes

$gg \to HHH$

PENTA1=3!=6
PENTA2=3!=6

BOX1=2*3=6
BOX2=3

TRI1=1
TRI2=3

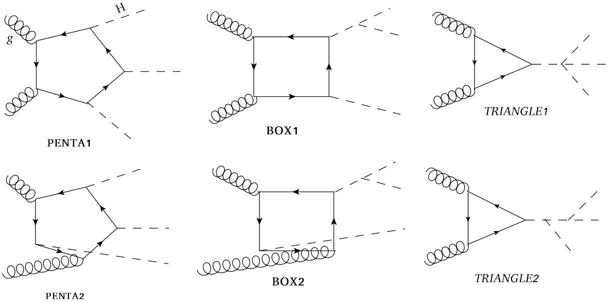

Figure : Different classes of diagrams contributing to GGHHH process. By commuting external legs, keeping one fixed, all the diagrams can be obtained. Some of the diagrams are related to the others by Furry's theorem, thereby reduces numerical computation.

Feynman Diagrams for Our Processes
$gg \to HHZ$

P1=4, # P2=4   # B1=4, # B2=2   # T1=1, # T2=1

P3=2, # P4=2   # B3=2, # B4=1   # T3=2

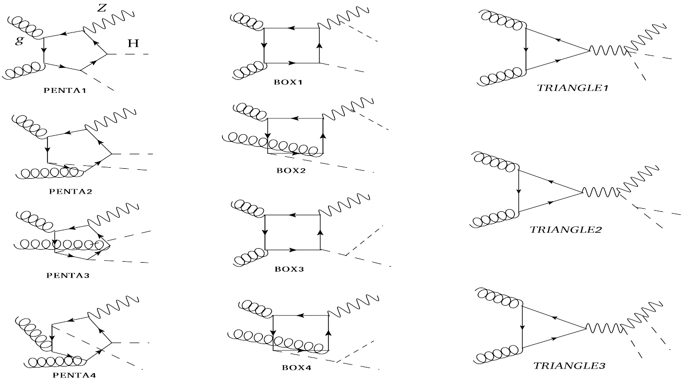

Figure : Different classes of diagrams contributing to GGHHZ process.

- let's take the example of PENTA1 diagram of $gg \to HHH$ process

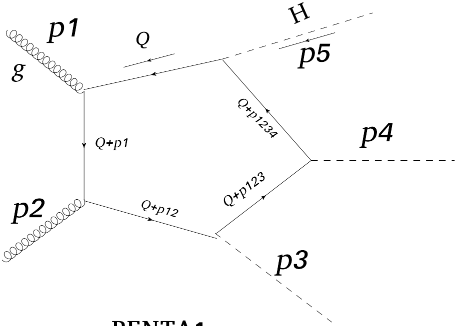

PENTA1

$$\mathcal{M} = \int \frac{d^4Q}{(2\pi)^4}\,\frac{\mathrm{Tr}[(\not{Q}+m)\not{\epsilon}_1(\not{Q}+\not{p}1+m)\not{\epsilon}_2(\not{Q}+\not{p}12+m)(\not{Q}+\not{p}123+m)(\not{Q}+\not{p}1234+m)]}{d_0\, d_1\, d_2\, d_3\, d_4}$$

where $d_0 = Q^2 - m^2$; $d_1 = (Q+p1)^2 - m^2$, and so on.

One loop reduction

Any one-loop amplitude can be reduced to only four type of master scalar integrals, i.e,

$$\mathcal{M}^{oneloop} = \sum_i \left(a_i A_0^i\right) + \sum_{i,j} \left(b_{i,j} B_0^{i,j}\right) + \sum_{i,j,k} \left(c_{i,j,k} C_0^{i,j,k}\right) + \sum_{i,j,k,l} \left(d_{i,j,k,l} D_0^{i,j,k,l}\right) + \mathcal{R}.$$

$$A_0^i = \int \frac{d^n Q}{(2\pi)^n} \frac{1}{d_i}, \quad B_0^{i,j} = \int \frac{d^n Q}{(2\pi)^n} \frac{1}{d_i\, d_j},$$

$$C_0^{i,j,k} = \int \frac{d^n Q}{(2\pi)^n} \frac{1}{d_i\, d_j\, d_k}, \quad D_0^{i,j,k,l} = \int \frac{d^n Q}{(2\pi)^n} \frac{1}{d_i\, d_j\, d_k\, d_l}.$$

$\mathcal{R}$ is the rational term coming during the tensor reduction due to the UV- regularization.

The techniques used to reduce the tensor integrals are:

- Passarino-Veltman technique
- Others
- Oldenborgh-Vermaseren technique

There are also techniques to reduce n-point scalar integral (where n$\geq$ 5) into master scalar integrals (A_0, B_0, C_0, D_0).

Anomalous interactions (BSM)

We are considering some anomalous interactions on top of the Standard Model interactions.

- $\mathcal{L}_{\bar{t}tH} = -\frac{m_t}{v}\bar{t}[(1 + y_t{}^V) + i y_t{}^A \gamma_5] t H \,.$
- $\mathcal{L}_{HHH} = -\frac{3m_H^2}{v}\left(\frac{1}{6}(1 + g_{3H}^{(1)})\, H^3 + g_{3H}^{(2)}\, \frac{H\partial_\mu H \partial^\mu H}{6m_H^2}\right)$

  $\mathcal{L}_{HHHH} = -\frac{3m_H^2}{v^2}\left(\frac{1}{24}(1 + g_{4H}^{(1)})\, H^4 + g_{4H}^{(2)}\, \frac{H^2\partial_\mu H \partial^\mu H}{24m_H^2}\right)$
- $$\mathcal{L}_{HZZ} = \frac{gM_z}{c_W}\left\{\frac{1}{2}(1 + g_{HZZ}^{(0)}) H Z_\mu Z^\mu - \frac{1}{4} g_{HZZ}^{(1)} \frac{H Z_{\mu\nu} Z^{\mu\nu}}{M_Z^2} - g_{HZZ}^{(2)}\, \frac{H Z_\nu \partial_\mu Z^{\mu\nu}}{M_Z^2}\right\}$$

  $$\mathcal{L}_{HHZZ} = \frac{gM_z}{c_W v}\left\{\frac{1}{4}(1 + g_{HHZZ}^{(0)})\, H H Z_\mu Z^\mu\right\}$$

$gg \to HHH$
SM

- The amplitude is found to be gauge invariant, UV finite, and IR finite .
- Scale: $\mu_R = \mu_F = \sqrt{\hat{s}}$.

$\sqrt{s}$ [TeV]	8	13	33	100
$\sigma_{GG}^{HHH,LO}$ [ab]	$7.0^{+34.6\%}_{-24.0\%}$	$32.0^{+30.6\%}_{-22.2\%}$	$330.8^{+23.8\%}_{-18.4\%}$	$3121.1^{+17.4\%}_{-14.1\%}$

Table : $pp \to HHH$ hadronic cross section.

$\sqrt{s}$ [TeV]	8	13	33	100
σ_{penta}^{HHH} [ab]	22.1	94.4	916.4	8067.8
σ_{box}^{HHH} [ab]	12.9	53.6	502.5	4287.4
$\sigma_{triangle}^{HHH}$ [ab]	0.8	3.5	32.1	270.8
σ_{total}^{HHH} [ab]	7.0	32.0	330.3	3121.3

Table : Interference effect in $gg \to HHH$.

$gg \to HHH$
SM

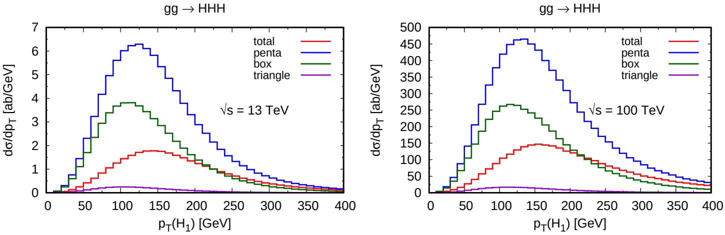

Figure : Interference in $gg \to HHH$ at 13 TeV and 100 TeV

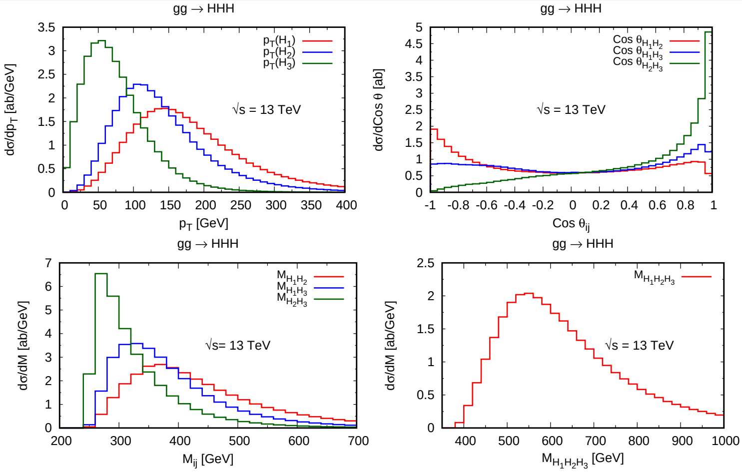

Figure : Kinematic distributions for GGHHH in the SM at 13 TeV. These plots are obtained after p_T ordering the Higgs bosons. H_1, H_2, and H_3 refer to the hardest, second hardest, and third hardest Higgs bosons in p_T respectively.

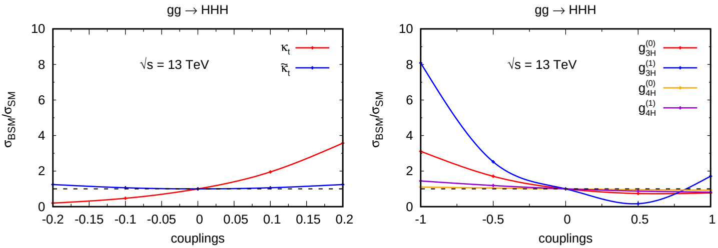

Figure : $\frac{\sigma_{\rm BSM}}{\sigma_{\rm SM}}$ as function of various Higgs anomalous couplings affecting GGHHH at 13 TeV.

$gg \to HHH$
SM vs BSM

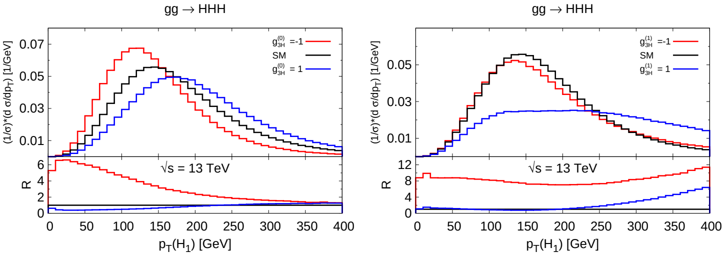

Figure : Normalized leading $p_T(H)$ distribution in $gg \to HHH$ at 13 TeV for some benchmark values of anomalous trilinear Higgs self-coupling. In the lower panels R is defined as the ratio of the distributions $(d\sigma/dp_T)$ in BSM and in SM.

- The amplitude is found to be gauge invariant, UV finite, and IR finite .
- Scale: $\mu_R = \mu_F = \sqrt{\hat{s}}$.
- Kinematic Cuts: $p_T^{H,Z} > 1\mathrm{GeV}$, $y^{H,Z} < 5$.

$\sqrt{s}$ (TeV)	8	13	33	100
$\sigma_{\mathrm{GG}}^{\mathrm{HHZ,\,LO}}$ [ab]	$10.0^{+34.0\%}_{-24.0\%}$	$42.3^{+30.9\%}_{-21.4\%}$	$406.7^{+23.9\%}_{-17.9\%}$	$3562.4^{+16.8\%}_{-13.9\%}$
$\sigma_{\mathrm{QQ}}^{\mathrm{HHZ,\,LO}}$ [ab]	$97.2^{+3.9\%}_{-3.8\%}$	$236.7^{+1.3\%}_{-1.5\%}$	$988.8^{+2.6\%}_{-3.3\%}$	$4393.0^{+7.1\%}_{-7.8\%}$
$\sigma_{\mathrm{QQ}}^{\mathrm{HHZ,\,NLO}}$ [ab]	$122.0^{+1.7\%}_{-1.6\%}$	$294.5^{+1.5\%}_{-1.0\%}$	$1197.0^{+1.7\%}_{-1.9\%}$	$4971.0^{+1.8\%}_{-3.2\%}$
$\mathrm{R}_1 = \frac{\sigma_{\mathrm{GG}}^{\mathrm{HHZ,\,LO}}}{\sigma_{\mathrm{QQ}}^{\mathrm{HHZ,\,LO}}}$	0.10	0.18	0.41	0.81
$\mathrm{R}_2 = \frac{\sigma_{\mathrm{GG}}^{\mathrm{HHZ,\,LO}}}{\sigma_{\mathrm{QQ}}^{\mathrm{HHZ,\,NLO}}}$	0.08	0.14	0.34	0.72
$\mathrm{R}_3 = \frac{\sigma_{\mathrm{GG}}^{\mathrm{HHZ,\,LO}}}{(\sigma_{\mathrm{QQ}}^{\mathrm{HHZ,\,NLO}} - \sigma_{\mathrm{QQ}}^{\mathrm{HHZ,\,LO}})}$	0.40	0.73	1.95	6.16

Table : A comparison of different order contribution to $pp \to HHZ$ hadronic cross section.

$gg \to HHZ$

SM

$\sqrt{s}$ (TeV)	8	13	33	100
σ^{HHZ}_{penta} [ab]	30.8	148.1	1718.4	17694.0
σ^{HHZ}_{box} [ab]	73.1	434.7	7468.2	115747.2
$\sigma^{HHZ}_{triangle}$ [ab]	78.4	475.6	8157.2	124273.1
σ^{HHZ}_{total} [ab]	10.0	42.3	406.4	3557.5

Table : Interference

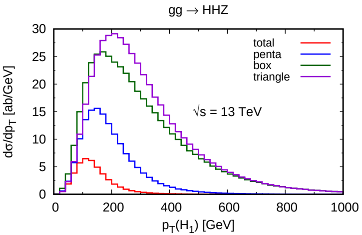

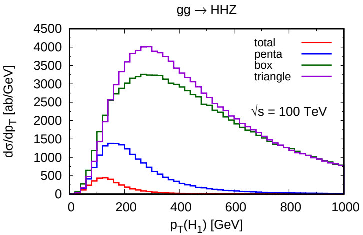

$gg \to HHZ$
SM

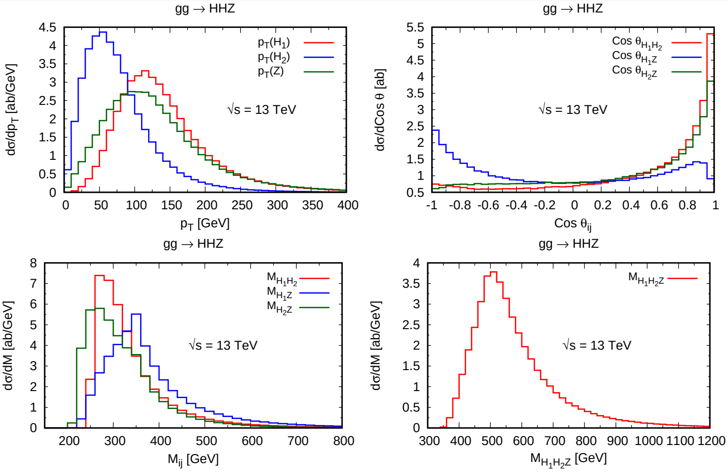

Figure : Kinematic distributions for $gg \to HHZ$ in the SM at 13 TeV. These plots are obtained after p_T ordering the Higgs bosons. H_1 and H_2 refer to the hardest and second hardest Higgs bosons in p_T respectively.

$pp \to HHZ$
SM

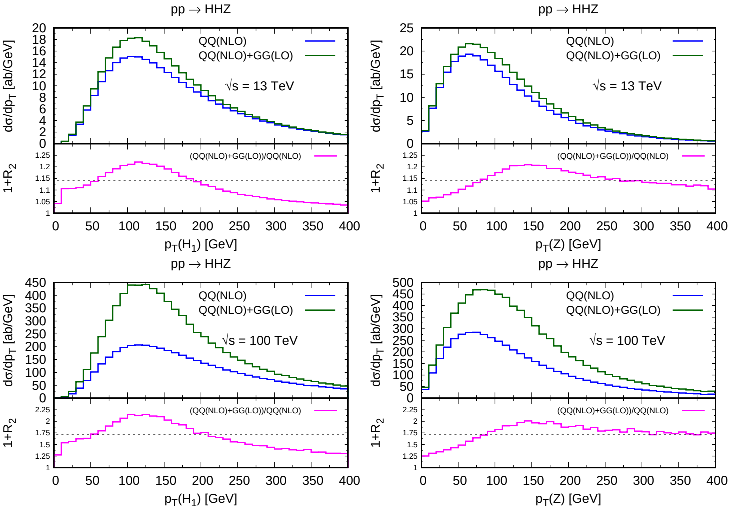

Figure : Combined $gg \to HHZ$(LO) + $qq \to HHZ$(NLO) contribution to $p_T(H_1)$ and $p_T(Z)$ distributions in the SM at 13 TeV and 100 TeV.

$gg \to HHZ$ SM

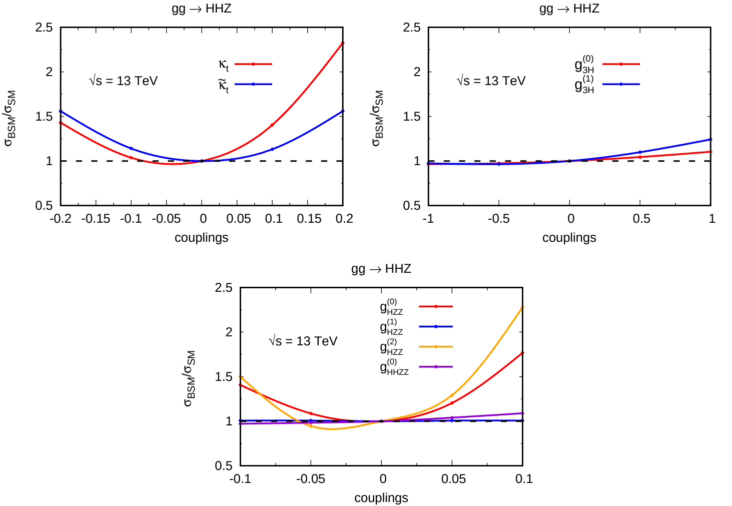

Figure : $\frac{\sigma_{\rm BSM}}{\sigma_{\rm SM}}$ as a function of anomalous couplings of the Higgs boson in $gg \to HHZ$ at 13 TeV.

$gg \to HHZ$

SM vs BSM

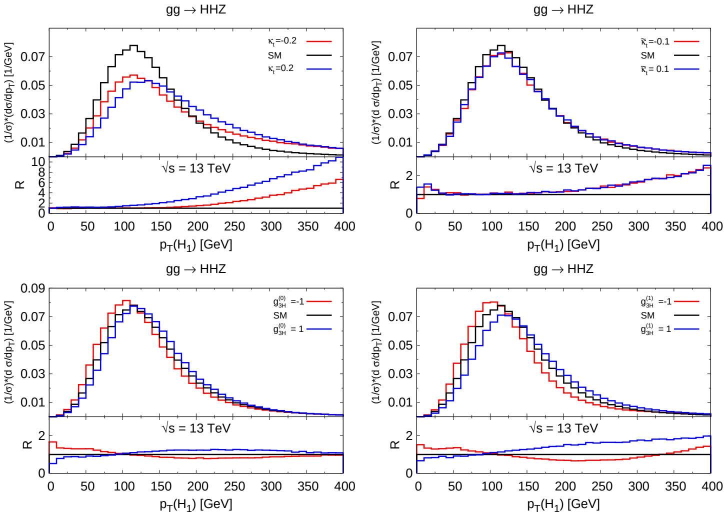

Figure : Normalized leading $p_T(H)$ distribution in $gg \to HHZ$ at 13 TeV for some benchmark values of anomalous couplings.

$gg \to HHZ$

SM vs BSM

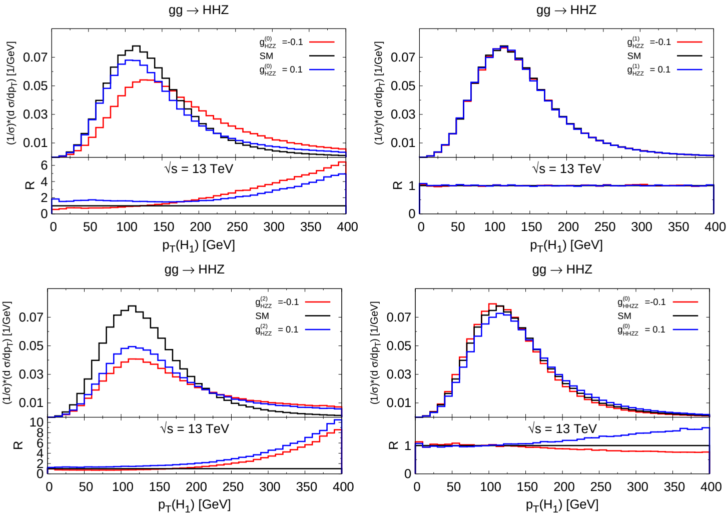

Figure : Normalized leading $p_T(H)$ distribution in $gg \to HHZ$ at 13 TeV for some benchmark values of *HZZ* and *HHZZ* anomalous couplings.

Summary and conclusions

- $gg \to HHH$ via 1-loop is the leading order process. There is no tree level diagram. It will be really difficult to detect HHH final states. Detection of it is crucial for Higgs potential determination.
- $gg \to HHH$ is sensitive to anomalous trilinear Higss boson self-coupling.
- To the process $PP \to HHZ$, contribution of $gg \to HHZ$ is NNLO in α_s. $gg \to HHZ$ is similar to the NLO contribution in $qq \to HHZ$ at currently running LHC, and can be six times larger at 100 TeV LHC because of larger gluon flux.
- $gg \to HHZ$ has some modest dependence on anomalous HZZ coupling.
- Observation of HHH and HHZ will require very high luminosity if there is no anomalous couplings. With increasing luminosity, complications due to more pile-up events will also arise.

Summary and conclusions

- To find traces and to simplify expressions further, FORM, a symbolic manipulation software, has been used.
- We have used Oldenborgh-Vermaseren tensor Reduction technique in our calculation.
- To find master scalar integrals, OneLOop package has been used.
- To handle numerical instability, contributions from exceptional phase-space points are excluded.

Thank You!

BACK UP SLIDES

- $B_\mu = \int \frac{d^nQ}{(2\pi)^n} \frac{Q_\mu}{(Q^2-m^2)((Q+p)^2-m^2)}$
- Obviously, this can be written as $B_\mu = p_\mu B_1$
- Now let's find B_1
-

$$\begin{aligned}
B_1 &= \frac{1}{p^2}\int \frac{d^nQ}{(2\pi)^n} \frac{Q\cdot p}{(Q^2-m^2)((Q+p)^2-m^2)} \\
&= \frac{1}{p^2}\int \frac{d^nQ}{(2\pi)^n} \frac{\frac{1}{2}\{(Q+p)^2-Q^2-p^2\}}{(Q^2-m^2)((Q+p)^2-m^2)} \\
&= \frac{1}{2p^2}\int \frac{d^nQ}{(2\pi)^n} \left[\frac{1}{(Q^2-m^2)} - \frac{1}{((Q+p)^2-m^2)} \right. \\
&\qquad \left. - \frac{p^2}{(Q^2-m^2)((Q+p)^2-m^2)}\right] \\
&= -\frac{1}{2}\int \frac{d^nQ}{(2\pi)^n} \frac{1}{(Q^2-m^2)((Q+p)^2-m^2)} = -\frac{1}{2}B_0
\end{aligned}$$

- Let's first define generalized Kronecker delta:

$$\delta^{\mu_1\mu_2}_{\nu_1\nu_2} = \begin{vmatrix} \delta^{\mu_1}_{\nu_1} & \delta^{\mu_1}_{\nu_2} \\ \delta^{\mu_2}_{\nu_1} & \delta^{\mu_2}_{\nu_2} \end{vmatrix} = \delta^{\mu_1}_{\nu_1}\delta^{\mu_2}_{\nu_2} - \delta^{\mu_1}_{\nu_2}\delta^{\mu_2}_{\nu_1} \; ;$$

$$\begin{aligned} \delta^{p_1 p_2}_{q_1 q_2} &= \delta^{\mu_1\mu_2}_{\nu_1\nu_2}\, p_{1\mu_1}\, p_{2\mu_2}\, q_1^{\nu_1}\, q_2^{\nu_2}. \\ &= (p_1\cdot q_1)(p_2\cdot q_2) - (p_1\cdot q_2)(p_2\cdot q_1)\,. \end{aligned}$$

- For any two linearly independent vectors q_1 and q_2, we can define two dual vectors u_1, and u_2 such that $u_i \cdot q_j = \delta_{ij}$.
- Now if we write $u_1 = a_1 q_1 + a_2 q_2$, then using this in the above we will get a matrix equation for a and b:

$$\begin{bmatrix} q_1\cdot q_1 & q_1\cdot q_2 \\ q_1\cdot q_2 & q_2\cdot q_2 \end{bmatrix} \begin{bmatrix} a_1 \\ a_2 \end{bmatrix} = \begin{bmatrix} 1 \\ 0 \end{bmatrix}.$$

- The above 2×2 matrix is known as Gram matrix of q_1 and q_2 , and its determinant is known as Gram determinant.

- Solving the matrix equation for a_1 and a_2, we will get $u_1^\mu = \frac{\delta^{\mu\ \ q_2}_{q_1 q_2}}{\delta^{q_1 q_2}_{q_1 q_2}}$. Similarly, $u_2^\mu = \frac{\delta^{q_1\ \ \mu}_{q_1 q_2}}{\delta^{q_1 q_2}_{q_1 q_2}}$. u_1 and u_2 are known as van Neerven-Vermaseren basis vectors.
- Using above expressions of u_1 and u_2, it can be shown that $\begin{bmatrix} u_1 \cdot u_1 & u_1 \cdot u_2 \\ u_1 \cdot u_2 & u_2 \cdot u_2 \end{bmatrix} = \begin{bmatrix} q_1 \cdot q_1 & q_1 \cdot q_2 \\ q_1 \cdot q_2 & q_2 \cdot q_2 \end{bmatrix}^{-1}$.
- For m linearly independent vectors $q_1, q_2, q_3, ..., q_m$, we will similarly get $u_1^\mu = \frac{\delta^{\mu\ \ q_2 q_3 \cdots q_m}_{q_1 q_2 q_3 \cdots q_m}}{\delta^{q_1 q_2 q_3 \cdots q_m}_{q_1 q_2 q_3 \cdots q_m}}$, and so on.

- The projective tensor is defined as

$$\omega_\nu^\mu = \frac{\delta^{q_1 q_2 \dots q_m \mu}_{q_1 q_2 \dots q_m \nu}}{\delta^{q_1 q_2 \dots q_m}_{q_1 q_2 \dots q_m}} = \left(\delta_\nu^\mu - \sum_{i=1}^{m} u_{i\nu} q_i^\mu \right) = \left(\delta_\nu^\mu - \sum_{i=1}^{m} u_i^\mu q_{i\nu} \right)$$

- ω_ν^μ holds these properties:

$$\omega_\nu^\mu q_{i_\mu} = \omega_\nu^\mu q_i^\nu = \omega_\nu^\mu u_{i_\mu} = \omega_\nu^\mu u_i^\nu = 0,\ \omega_\nu^\mu \omega_\rho^\nu = \omega_\rho^\mu, \text{and } \omega_\mu^\mu = n-m$$

- using the def^n of ω_ν^μ, we have $\delta_\nu^\mu = \left(\sum_{i=1}^m u_i^\mu q_{i\nu} + \omega_\nu^\mu\right)$
- so $\boxed{Q^\mu = \left(\sum_{i=1}^m u_i^\mu Q \cdot q_i + \omega_Q^\mu\right)}$, van Neerven Vermaseren decomposition .

- $C^\mu = \int \frac{d^nQ}{(2\pi)^n} \frac{Q^\mu}{(Q^2-m^2)((Q+q_1)^2-m^2)((Q+q_2)^2-m^2)}$
- Using $\boxed{Q^\mu = \left(\sum_{i=1}^{m} u_i^\mu Q\cdot q_i + \omega_Q^\mu\right)}$, we have

$$
\begin{aligned}
C^\mu &= \int \frac{d^nQ}{(2\pi)^n} \frac{\left(\sum_{i=1}^{2} u_i^\mu Q\cdot q_i + \omega_Q^\mu\right)}{(Q^2-m^2)((Q+q_1)^2-m^2)((Q+q_2)^2-m^2)} \\
&= \int \frac{d^nQ}{(2\pi)^n} \frac{\left(\sum_{i=1}^{2} (u_i^\mu)(Q\cdot q_i)\right)}{(Q^2-m^2)((Q+q_1)^2-m^2)((Q+q_2)^2-m^2)}
\end{aligned}
$$

- In the above, ω_Q^μ term gives zero as the integration can depend only on q_1^μ and q_2^μ .
- (u_i^μ) is one of the source of numerical instability .